

## Pyrolysis and fire behaviour of epoxy resin composites based on a phosphorus-containing polyhedral oligomeric silsesquioxane (DOPO-POSS)

Wenchao Zhang, Xiangmei Li, Rongjie Yang\*

National Laboratory of Flame Retardant Materials, School of Materials, Beijing Institute of Technology, 5 South Zhongguancun Street, Haidian District, Beijing 100081, PR China

### ARTICLE INFO

#### Article history:

Received 11 February 2011

Received in revised form

9 May 2011

Accepted 11 July 2011

Available online 20 July 2011

#### Keywords:

Epoxy resin

Pyrolysis

Flame retardancy

POSS

DOPO

### ABSTRACT

The pyrolysis and fire behaviour of epoxy resin (EP) composites based on a novel polyhedral oligomeric silsesquioxane containing 9,10-dihydro-9-oxa-10-phosphaphenanthrene-10-oxide (DOPO-POSS) and diglycidyl ether of bisphenol A (DGEBA) have been investigated. The pre-reaction between the hydroxyl groups of DOPO-POSS and the epoxy groups of DGEBA at 140 °C is confirmed by FTIR, which means that DOPO-POSS molecules of hydroxyl group could easily disperse into the epoxy resin at the molecular level. The EP composites with the DOPO-POSS were prepared through a curing agent, m-phenylenediamine (m-PDA). The morphologies of the EP composites observed by SEM indicate that DOPO-POSS disperses with nano-scale particles in the EP networks, which implies good compatibility between them. The thermal properties and pyrolysis of the EP composites were analyzed by DSC and TGA, TGA-FTIR, and TGA-MS. The analysis indicates that the DOPO-POSS change the decomposition pathways of the epoxy resin and increase its residue at high temperature; moreover, the release of phosphorous products in the gas phase and the existence of Si–O and P–O structures in the residue is noted. The fire behaviour of the EP composites was evaluated by cone calorimeter (CONE). The CONE tests show that incorporation of DOPO-POSS into epoxy resin can significantly improve the flame retardancy of EP composites. SEM and XPS were used to explore micro-structures and chemical components of the char from CONE tests of the EP composites, they support the view that DOPO-POSS makes the char strong with the involvement of Si–O and P–O structures.

© 2011 Elsevier Ltd. All rights reserved.

### 1. Introduction

Epoxy resins are very important thermosetting materials owing to their excellent mechanical and chemical properties [1–3]. They are widely applied as advanced composite matrices in electronic/electrical industries where a remarkable flame-retardant grade is required, but the fire risk is a major drawback of these materials [4]. Recently the research efforts on epoxy resins have been focused on improving their thermal stability, increasing glass transition temperatures and enhancing flame retardancy [1,5–7]. Traditionally, halogenated compounds are widely used as co-monomers or additive with epoxy resins to obtain fire-retardant materials. However, flame-retardant epoxy resins containing bromine or chlorine can produce poisonous and corrosive smoke and may give super toxic halogenated dibenzodioxins and dibenzofurans [4]. Because of environmental concerns, some halogen-containing

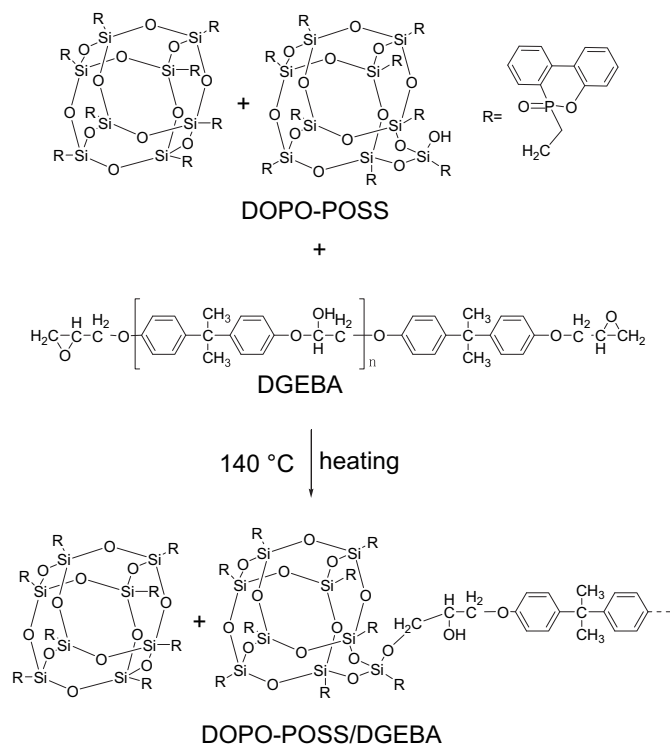
flame retardants that have high flame-resistant efficiencies have been gradually prohibited [8,9].

Organic–inorganic hybrid composites are typically considered a new generation of high-performance materials, as they combine the advantages of inorganic materials with those of organic polymers [10–13]. Polyhedral oligomeric silsesquioxanes (POSS) have the chemical composition (RSiO<sub>1.5</sub>), where R is hydrogen or any alkyl, alkylene, aryl, or arylene group, or organo-functional derivatives thereof, similar to the compositions of both silica (SiO<sub>2</sub>) and silicone (R<sub>2</sub>SiO) [14,15]. POSS molecules with a nanosized, cage-shaped, three-dimensional structure can be incorporated into almost all kinds of thermoplastic or thermosetting polymers to improve their thermal properties and oxidation resistance and flame retardancy [16–19].

Phosphorous compounds could impart flame retardancy through flame inhibition in the gas phase and char enhancement in the condensed phase [4,20–22]. Several either nonreactive or reactive phosphorus-containing flame retardants in epoxy resins have been investigated in recent research articles [23–26]. 9,10-dihydro-9-oxa-10-phosphaphenanthrene-10-oxide (DOPO) is

\* Corresponding author. Tel.: +86 10 6891 2927.

E-mail address: [yryj@bit.edu.cn](mailto:yryj@bit.edu.cn) (R. Yang).



**Scheme 1.** Reaction process between DOPO-POSS and DGEBA.

a cyclic phosphate with a diphenyl structure, which has high thermal stability, good oxidation and water resistance [27–30]. Using DOPO or its derivatives as flame retardant, significant improvement in the fire behaviour of epoxy resins has been reported [23–26].

In our previous work [31,32], we described the successful synthesis of DOPO-containing polyhedral oligomeric silsesquioxane (DOPO-POSS) (Scheme 1). It is a novel phosphorus-containing POSS with high thermal stability, which may be an efficient halogen-free flame-retardant system for epoxy resin. In this article, flame retardancy and thermal degradation mechanism of epoxy resin composites based on the DOPO-POSS have been studied.

## 2. Experimental

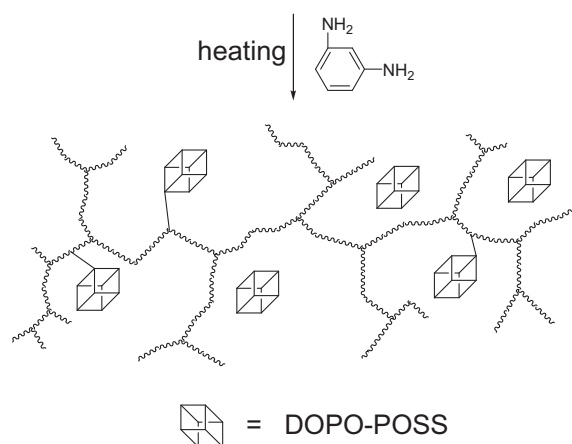
### 2.1. Materials

Diglycidyl ether of bisphenol A (DGEBA, E-44, epoxy equivalent = 0.44 mol/100 g) was purchased from FeiCheng DeYuan Chemicals CO., LTD. m-Phenylenediamine (m-PDA) was purchased from Tianjin GuangFu Fine Chemical Research Institute. DOPO-POSS was synthesized in our laboratory [31,32]. DOPO-POSS was mixture of perfect T<sub>8</sub> cage and imperfect T<sub>9</sub> cage with one Si–OH group on it.

**Table 1**  
Compositions of EP/DOPO-POSS composites.

Materials	EP control	EP-1	EP-2	EP-3
DGEBA (g)	100.0	100.0	100.0	100.0
m-Phenylenediamine (g)	12.0	12.0	12.0	12.0
DOPO-POSS (g)	0	5.89	12.44	28.00
DOPO-POSS (wt%)	0	5	10	20

### DOPO-POSS/DGEBA + DGEBA



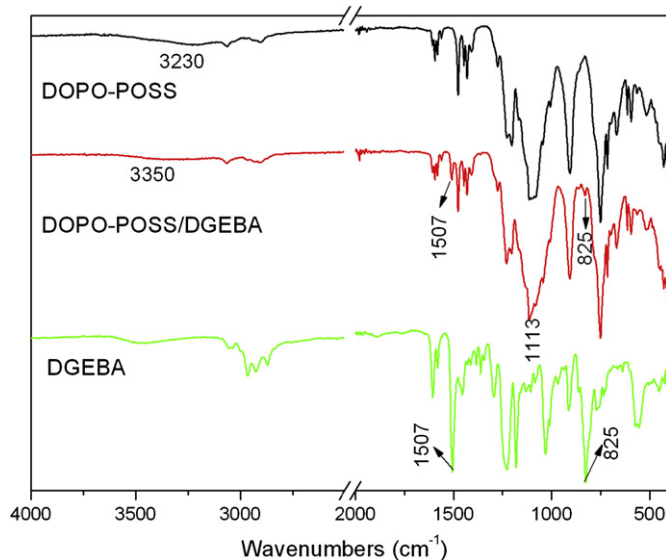
**Scheme 2.** Preparation of EP composites.

### 2.2. Synthesis of DOPO-POSS/DGEBA

The Si–OH group in DOPO-POSS is expected to react with the epoxide group in the DGEBA. The pre-reaction between DOPO-POSS and epoxy resin may enhance the compatibility of them. First, 28 g of DOPO-POSS and 100 g DGEBA were mixed in a three-necked flask. The temperature of the reaction mixture was raised to 140 °C and held at that temperature for 2 h. After that, the mixture was added into ethyl acetate. The resulting DOPO-POSS/DGEBA was obtained as a white powder after suction filtration. The synthesis process is illustrated in Scheme 1.

### 2.3. Preparation of EP composites

To realize pre-reaction between DOPO-POSS and epoxy resin, all of the DOPO-POSS was dispersed in DGEBA at 140 °C for 2 h before the curing. The contents of the DOPO-POSS in the EP composites were adjusted to be 5, 10, and 20 wt.%. After the system cooling to 70 °C, the curing agent (m-PDA) was then added. The equivalent weight ratio of DGEBA to m-PDA was 25:3, which are listed in Table 1. The mixtures were cured at 80 °C for 2 h and post-cured at



**Fig. 1.** FTIR spectra of DOPO-POSS, DGEBA, and DOPO-POSS/DGEBA.

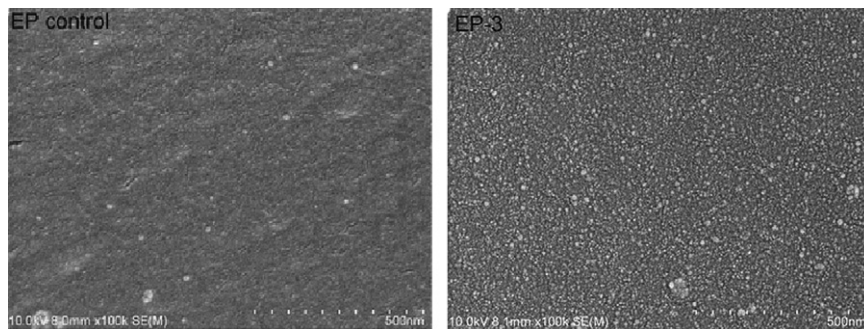


Fig. 2. SEM micrographs of EP control and EP-3.

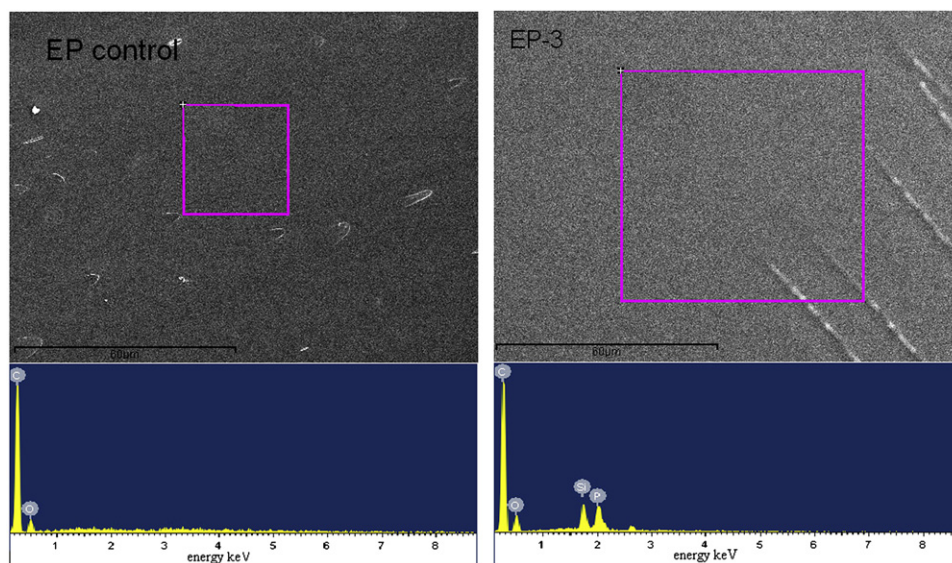


Fig. 3. EDXS spectrum of EP control and EP-3.

150 °C for 2 h. The curing process and structure of EP composites are shown in Scheme 2.

2.4. Measurements

Fourier transform infrared (FTIR) spectra were recorded on a NICOLET 6700 IR spectrometer. The detection mode is ATR. The

spectra were collected at 32 scans with a spectral resolution of 4 cm<sup>-1</sup>.

Thermal gravimetric analysis (TGA) was performed with a Netzsch 209 F1 thermal analyzer. The measurements were carried out under nitrogen atmosphere at a heating rate of 20 K/min from

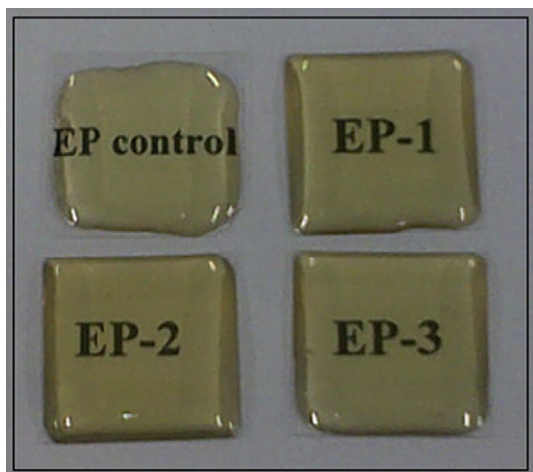


Fig. 4. Photographs of EP composites.

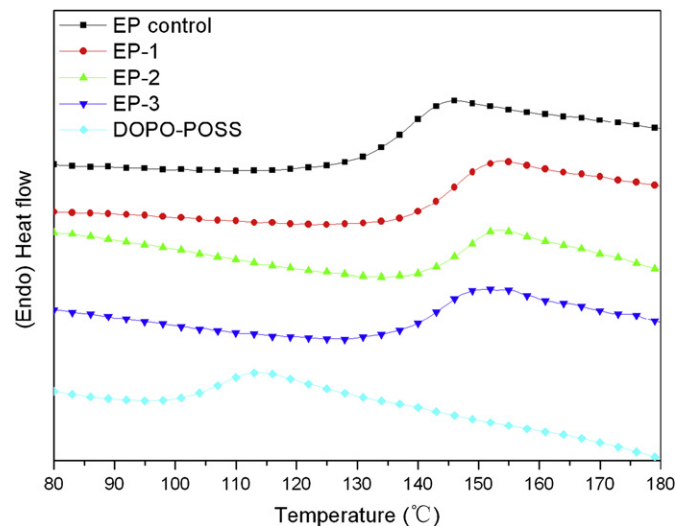


Fig. 5. DSC curves of EP composites.



**Table 2**  
TGA and DSC data of DOPO-POSS and EP/DOPO-POSS composites.

Samples	$T_g$ (°C)	$T_{onset}$ (°C)	$T_{max}$ (°C)	Residues at 800 °C (%)
DOPO-POSS	106.6	334	479	40.6
EP control	137.9	372	390	11.6
EP-1	145.6	360	391	13.0
EP-2	146.6	359	394	16.1
EP-3	142.7	362	442	20.9

40 °C to 800 °C. Typical results from TGA were reproducible within  $\pm 1\%$ , and the reported results are the average of three measurements. To detect gas species, the TGA was coupled with Fourier transform infrared spectrometry (TGA-FTIR, Nicolet 6700), and the measurements were carried out under nitrogen atmosphere at a heating rate of 20 K/min from 40 °C to 800 °C. The sample weight was 10 mg for each measurement.

DSC curves of the EP composites were measured using a Netzsch 204 F1 differential scanning calorimeter with a pressure cell. Samples (5–10 mg) were tested at a heating rate of 10 °C/min and results from the second heating in the range 25–250 °C are reported. Typical results from DSC were reproducible within  $\pm 1\%$ , and the reported results are the average of three measurements.

TGA/MS characterization was performed on a Netzsch STA 449 C–QMS 403 C instrument. TGA was performed in argon of high purity at a flow rate of 25 ml/min. In the experiment, a sample weighing approximately 10 mg was heated also at 20 °C/min from

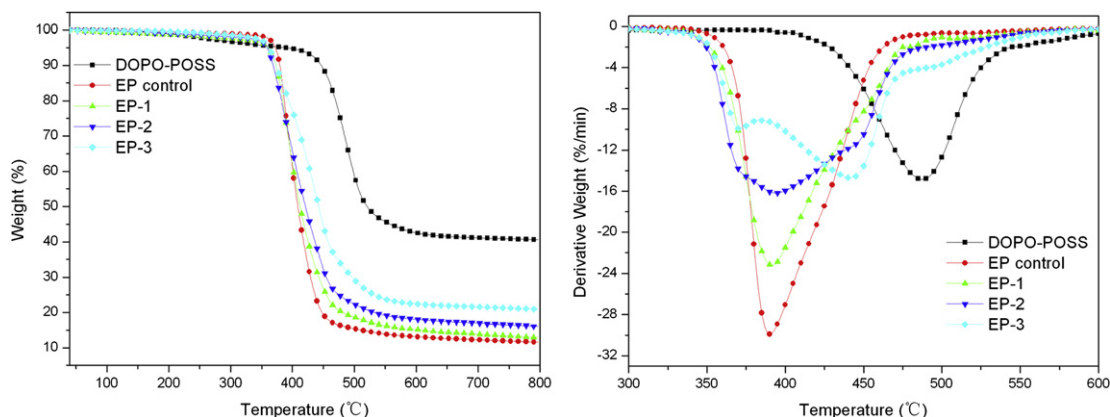
40 °C to 800 °C. Mass analysis was carried out using a spectrometer with an electron-impact ion source (70 eV); energy scanning was carried out in the range  $m/z$  10–110 at a rate of 0.2/s for each mass unit. The connection between TGA and MS was done by means of a quartz capillary at 200 °C.

To investigate the condensed phase of the EP composites, the residues corresponding to certain weight-loss in TGA measurement were obtained by stopping the test and cooling the samples. Then they were analyzed through FTIR (Nicolet 6700).

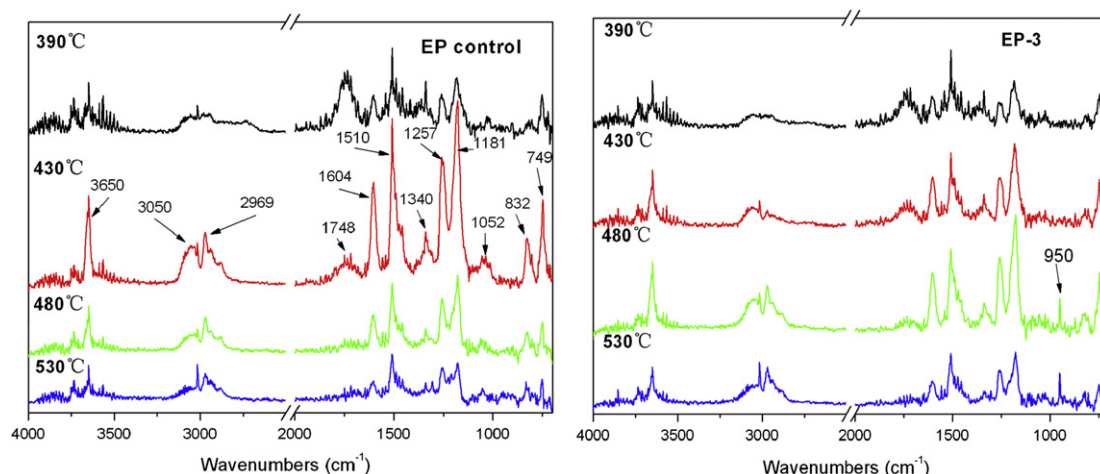
Scanning electron microscopy (SEM) experiments were performed with a Hitachi S-4800 scanning electron microscope. Samples (in morphological section) for SEM were prepared by low-temperature fracturing and sputtering the surface with gold. The C, O, Si, and P elements in the residue were verified by an energy dispersive X-ray spectroscopy (EDXS EX-350) in the SEM (Hitachi S-4800). Samples (in char analysis section) for SEM were the residue after the cone calorimeter test and sputtering the surface with gold.

Cone calorimeter measurements were performed at an incident radiant flux of 50 kW/m<sup>2</sup>, according to ISO 5660 protocol, using a Fire Testing Technology apparatus with a truncated cone-shaped radiator. The specimen (100 × 100 × 3 mm<sup>3</sup>) was measured horizontally without any grids. Typical results from cone calorimeter were reproducible within  $\pm 10\%$ , and the reported results are the average of three measurements.

The X-ray photoelectron spectroscopy (XPS) data were obtained using a Perkin–Elmer PHI 5300 ESCA system at 250 W (12.5 kV at



**Fig. 6.** TGA and DTG curves of DOPO-POSS and EP/DOPO-POSS composites in the nitrogen atmosphere.



**Fig. 7.** FTIR spectra of pyrolysis products of EP control and EP-3 at different temperatures.

**Table 3**  
Assignment of FTIR spectra of pyrolysis gases of EP control and EP-3.

Wavenumber (cm <sup>-1</sup> )	Assignment
3650	O–H stretching vibration of C <sub>Ar</sub> –OH or water
3050	C <sub>Ar</sub> –H stretching vibration of styrene derivatives
3016	Methane
2969	R–CH <sub>2</sub> –R, R–CH <sub>3</sub> stretching vibration of aliphatic components
1748	C=O stretching vibration of compounds containing carbonyl
1604, 1510, 1340	Aromatic rings vibration
1257, 1181, 1052	C–O stretching vibration
950	Ethylene
832, 749	C <sub>Ar</sub> –H deformation vibration

20 mA) under a vacuum better than 10<sup>-6</sup> Pa (10<sup>-8</sup> Torr). The char residues are obtained from the cone calorimeter tests. Typical results from XPS were reproducible within ±3%, and the reported results are the average of three measurements.

### 3. Results and discussion

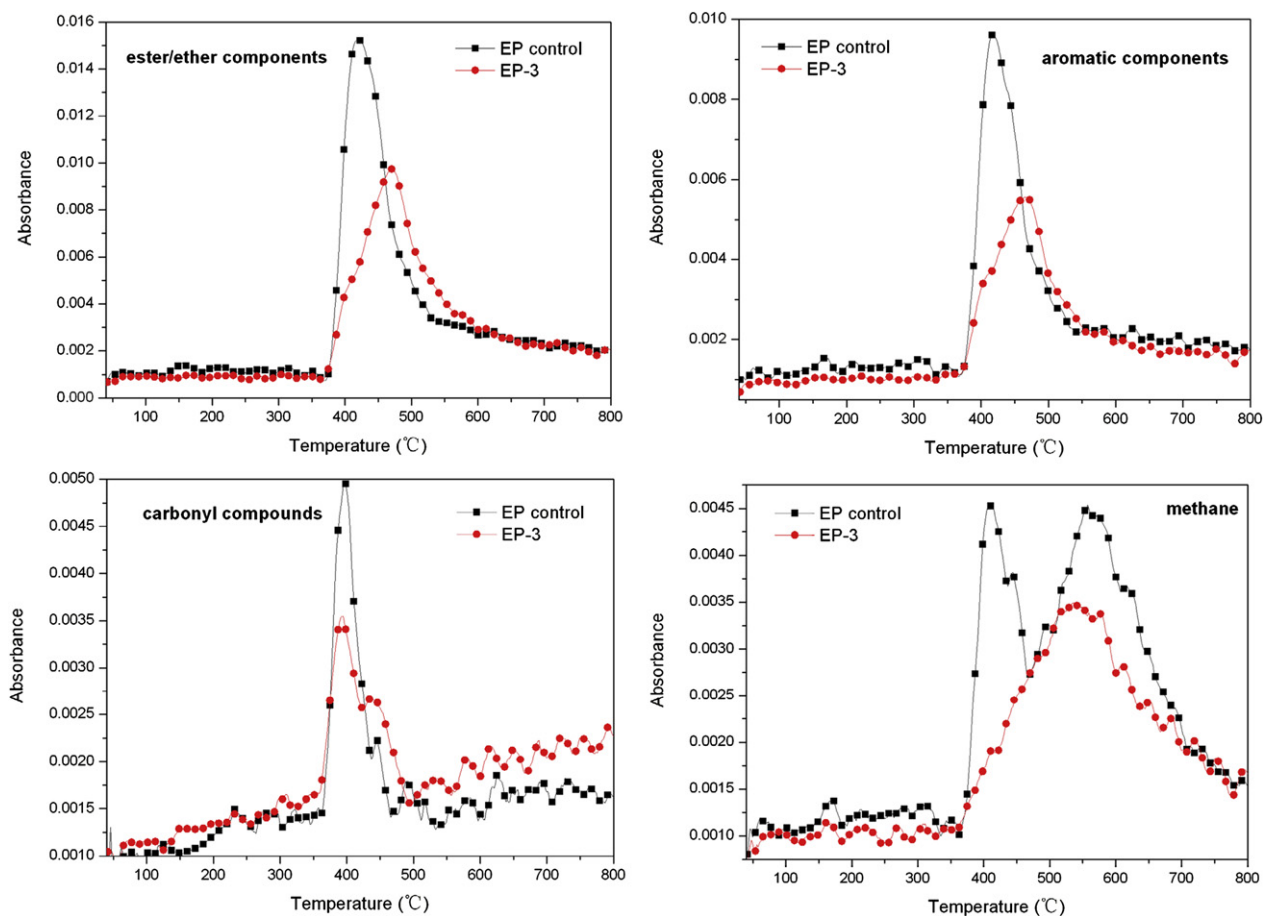
#### 3.1. FTIR analysis of the reaction processes

Infrared spectroscopy was performed to characterize the structures of the composites via the ring-opening reaction between the epoxide group of epoxy resin and the Si–OH functional group of the DOPO-POSS. Scheme 1 shows the reaction process and the

structure of DOPO-POSS/DGEBA. Fig. 1 presents FTIR curves of DOPO-POSS, DGEBA, and DOPO-POSS/DGEBA. The characteristic peak of the Si–O–Si group of DOPO-POSS is at 1060–1130 cm<sup>-1</sup>. The change of the shape of FTIR spectra in this range for DOPO-POSS/DGEBA demonstrates the occurrence of the reaction between Si–OH and epoxy ring [5]. In the curve of DOPO-POSS/DGEBA, the vibration of aromatic ring in DGEBA at 1507 cm<sup>-1</sup> and 825 cm<sup>-1</sup> were observed. Moreover, the hydroxyl group in DOPO-POSS at 3230 cm<sup>-1</sup> has disappeared, and a new hydroxyl group is formed at 3350 cm<sup>-1</sup>, meaning that the DOPO-POSS has reacted with the epoxy resin [5,10]. Connections are created between the organic and inorganic phases by covalent bonds. These covalent bonds could enhance the compatibility of DOPO-POSS and DGEBA.

#### 3.2. Morphological properties of EP composites

The morphology of the fractured EP composites surface was observed by SEM. In Fig. 2, the uniformly dispersed of DOPO-POSS particles were observed in the morphology of EP-3. As seen from the image of EP-3 in Fig. 2, majority of the DOPO-POSS particles are in the size range 10–50 nm. Fig. 3 shows an EDXS spectrum of EP control and EP-3. The Si and P element were observed in the EDXS spectrum of EP-3. The compatibility of DOPO-POSS molecules in epoxy resin is the key to achieving a well dispersed EP composite. Moreover, the enhanced dispersion can be attributed to the existence of covalent bonds between DOPO-POSS and DGEBA. Some DOPO-POSS molecules can easily disperse into the epoxy resin at



**Fig. 8.** Gas releases with time according to TG-FTIR spectra of EP control and EP-3: ester/ether components (1181 cm<sup>-1</sup>), aromatic components (1603 cm<sup>-1</sup>), carbonyl compounds (1743 cm<sup>-1</sup>), and methane (3016 cm<sup>-1</sup>).

the molecular level, which may result in composite properties that are very different from those of conventional polymer composites.

Fig. 4 presents pictures of EP composites with different DOPO-POSS contents. As can be seen from these photographs, the EP composites exhibit excellent optical transparency, which is very important characteristic for their application as protective coatings. This result is attributed to the well dispersion of DOPO-POSS, whose particles are smaller than the wavelength of visible light, in EP composites.

### 3.3. Thermal properties of EP composites

The glass transition temperature ( $T_g$ ) of the EP composites is measured by DSC. The DSC curves of all the samples are displayed in Fig. 5 and the results are summarized in Table 2. It is of interest to point out that only a glass transition was identified for these EP composites with 5, 10, and 20 wt.% DOPO-POSS compositions; moreover, the DOPO-POSS/EP composites exhibit a higher  $T_g$  than the EP control. These would be attributed to the reaction between the DOPO-POSS and DGEBA; thus, the rigid structures of DOPO-POSS clusters, which act as an anchoring point, are introduced to the composites. Moreover, the nano-dispersion of DOPO-POSS in EP composites may be another reason for unique  $T_g$  of each DOPO-POSS/EP composites. Otherwise,  $T_g$  of EP-3 is lower than that of other DOPO-POSS/EP composites. This would be attributed to the feature of low  $T_g$  of DOPO-POSS is more obvious with growing of DOPO-POSS content.

Thermal stabilities of the EP composites are evaluated by TGA. TGA and DTG curves of DOPO-POSS and the EP composites are

presented in Fig. 6. The relevant thermal decomposition data, including the  $T_{\text{onset}}$ , defined as the temperature at 5% weight-loss, the  $T_{\text{max}}$  defined as the temperatures at maximum weight-loss rate, and the char residues at 800 °C, are given in Table 2.

Compared with the EP control, the DOPO-POSS/EP composites exhibit lower  $T_{\text{onset}}$  with increase of DOPO-POSS load, which results from the initial degradation of the DOPO-POSS at relatively low temperature. However, the temperatures at maximum weight-loss rate are higher than that of the EP control, and the  $T_{\text{max}}$  of DOPO-POSS/EP composites enhance with increment of DOPO-POSS content. It is noticed that the residues of three DOPO-POSS/EP composites increase with DOPO-POSS load and the curve of EP-3 is quite different from curves of EP-1 and EP-2, moreover, the  $T_{\text{max}}$  of EP-3 is 48 °C higher than EP-2. It is reported that some POSS usually as a synergist can significantly reduce the flammability of polymers and increase char yields. The chemical bonding retains silicon in the condensed phase is an essential process that led to the formation of a glassy char and acts as a barrier to heat and mass transfer [5,10]. These results indicate that the interaction between DOPO-POSS and epoxy resin not only increases the weight-loss temperature at the rapid degradation region but also results in a high char yield.

### 3.4. Analysis of volatile pyrolysis products of EP composites

#### 3.4.1. TGA-FTIR analysis

Fig. 7 is the FTIR spectra of EP control and EP-3 at special temperature and the assignment of the absorption peaks are presented in Table 3. The major pyrolysis gases detected from the

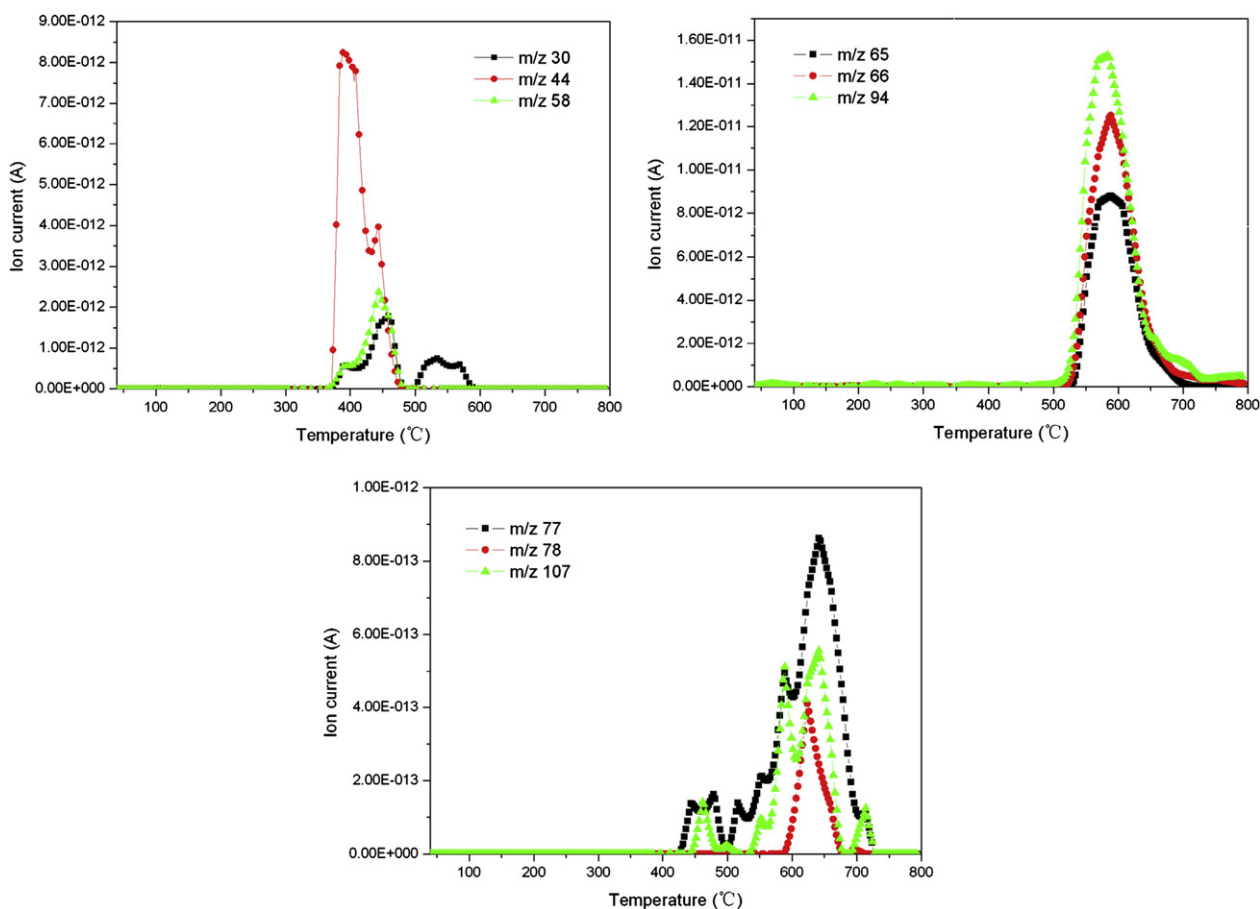


Fig. 9. Ion current curves for species produced from degradation of EP control.

decomposition process of EP control and EP-3 are phenol derivatives/water ( $3650\text{ cm}^{-1}$ ), aromatic components ( $3036$ ,  $1604$ ,  $1510$ , and  $1340\text{ cm}^{-1}$ ), aliphatic components ( $3016$ ,  $2972$ , and  $2869\text{ cm}^{-1}$ ) and ester/ether components ( $1257$ ,  $1181$ , and  $1052\text{ cm}^{-1}$ ), which corresponds well with the literatures [1,6]. As shown in Fig. 7 and Table 3, the evolving gas species for EP-3 are similar to that for EP control, except for ethylene at  $950\text{ cm}^{-1}$ . No other characteristic absorption of the gas products of DOPO-POSS were found in the FTIR spectra of EP-3 in Fig. 7. It implies that most of the decomposition products of DOPO-POSS remain in the condensed phase. This phenomenon might be attributed to the interactions between DOPO-POSS and EP networks.

Releases of the ester/ether components, aromatic components, carbonyl compounds, and methane as a function of temperature are shown in Fig. 8 according to their absorbance intensities in TG-FTIR spectra of EP control and EP-3.

As shown in Fig. 8, the initial decomposition temperature of EP-3 is similar to that of EP control, which corresponds well with the thermal analysis section. The thermal decomposition of EP control and EP-3 start with the evolution of carbonyl compounds, moreover, the release process is similar too. Although the initial release temperature of ester/ether components and aromatic components are same in Fig. 8, the quick release temperature is quite different. The quick release temperature of ester/ether components and aromatic components are enhanced with the DOPO-POSS load. It can be interpreted that DOPO-POSS could improve thermal stabilities of the DOPO-POSS/EP composites. The release of methane during the thermal decomposition of EP control has two main steps, whereas that of EP-3 is in only one step. The first quick

release peak of methane in the thermal decomposition process of EP control disappeared totally. This may be attributed to the covalent incorporation of DOPO-POSS into the epoxy resin.

Furthermore, the absorbance intensity of ester/ether components, aromatic components, carbonyl compounds, and methane of EP-3 are lower than that for EP control. The change in the evolved gases corresponds to the increase of char, because fewer volatiles such as styrene derivatives and aromatic ether/ester were produced through decomposition of EP-3 [33].

### 3.4.2. TGA-MS analysis

TG-FTIR measurement investigates only the functional group information about the pyrolysis products, exact composition of the pyrolysis products can be established by mass spectroscopy. The exact compositions of the EP control and EP-3 degradation products were determined by thermogravimetry coupled to a mass spectrometer. The volatilization profiles, represented as ion current, of the fragments originating in the thermal degradation of EP composites are shown in Figs. 9 and 10. The possible structural assignments of that are listed in Table 4.

It can be observed from Figs. 9 and 10 that intensive signals of the species with different ratios of mass to charge ( $m/z$ ) appear within the two temperature ranges. CO and ethylene can be determined by the  $m/z$  28, formaldehyde can be determined by the  $m/z$  30, acetaldehyde and  $\text{CO}_2$  can be determined by the  $m/z$  44, and acetone can be determined by the  $m/z$  58. These are released within the temperature range of  $350\text{--}500\text{ }^\circ\text{C}$ . The beginnings of the thermal decomposition of EP composites are the release of carbonyl compounds which corresponds well with the TG-FTIR analysis

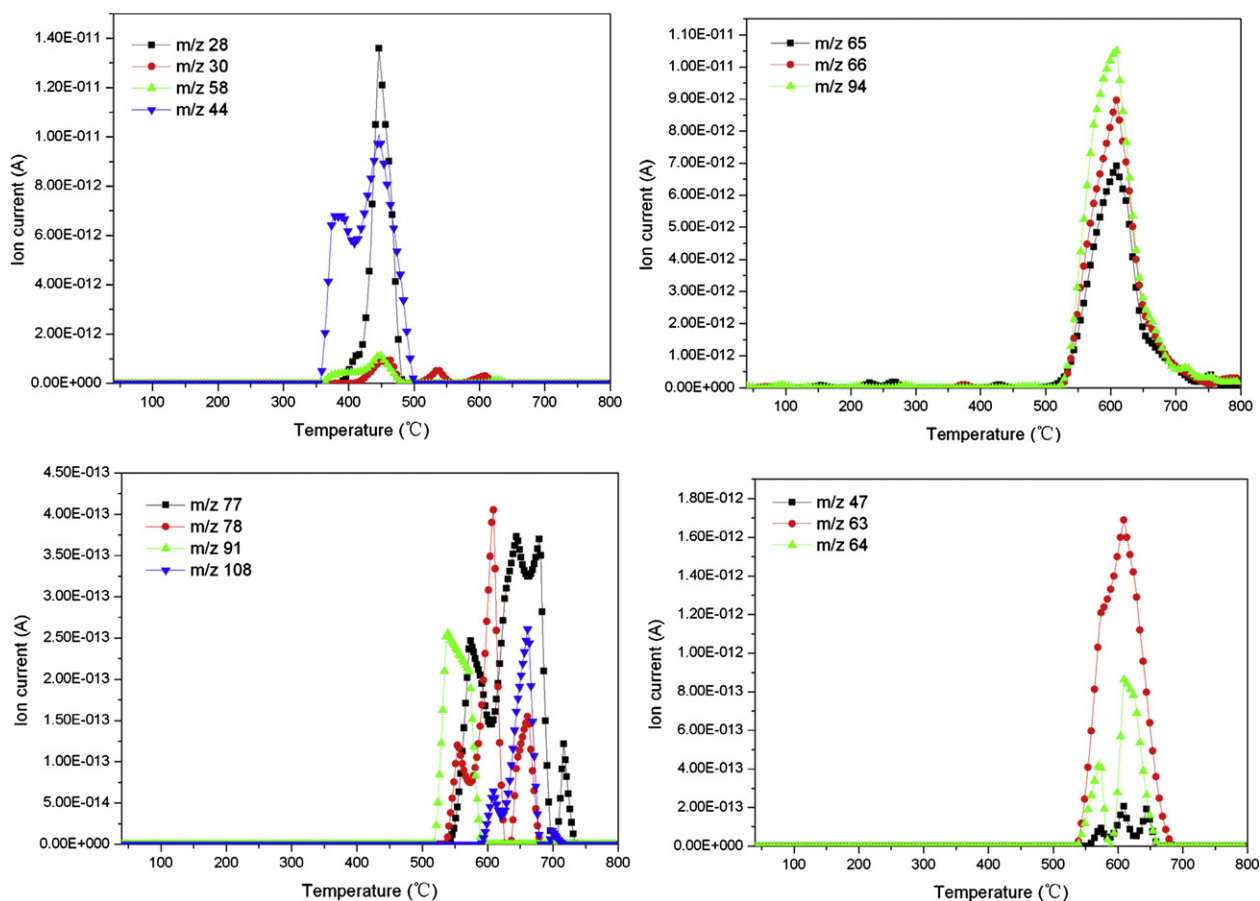

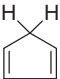
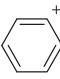
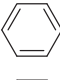
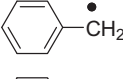
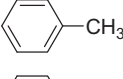

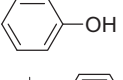


Fig. 10. Ion current curves for species produced from degradation of EP-3.

**Table 4**  
Possible structural assignments in the TG-MS of EP-3.

<i>m/z</i>	Structures	<i>m/z</i>	Structures
15	•CH <sub>3</sub>	64	HO <sub>2</sub> P <sup>+</sup>
28	CO	65	
28	CH <sub>2</sub> =CH <sub>2</sub>	66	
30	O=CH <sub>2</sub>	74	$\bullet \text{O}-\text{H}_2\text{C}-\overset{\text{OH}}{\underset{\text{H}}{\text{C}}}-\text{CH}_2$
44	CO <sub>2</sub>	77	
44	H <sub>3</sub> C-CH=O	78	
46	CH <sub>3</sub> -CH <sub>2</sub> -OH or H <sub>3</sub> C-O-CH <sub>3</sub>	91	
47	OP <sup>+</sup>	92	
51		94	
58	H <sub>3</sub> C-C=O-CH <sub>3</sub>	107	$\text{H}_2\text{C}^+-\text{C}_6\text{H}_4-\text{OH}$
63	O <sub>2</sub> P <sup>+</sup>	108	$\text{H}_3\text{C}-\text{C}_6\text{H}_4-\text{OH}$

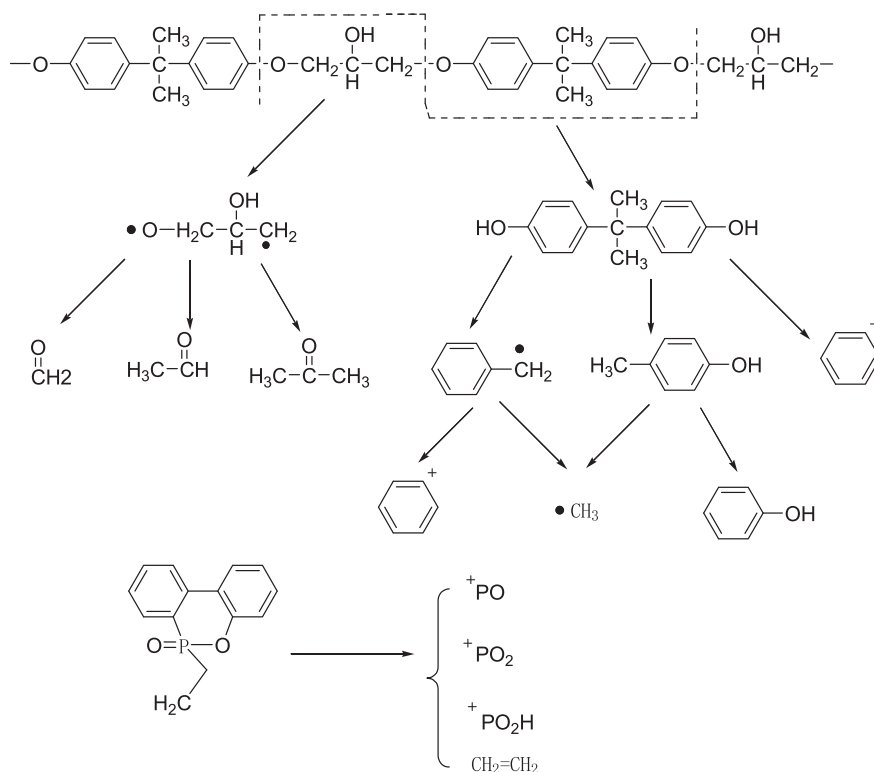
section. The Fragments of *m/z* 65, 66, 77, 78, 91 and 92 belong to aromatic components. Phenol (*m/z* 94) and methyl phenol (*m/z* 107, 108) can be also identified. These are released within the temperature range of 500–650 °C, which is little higher than that of the degradation stage described in the TGA-FTIR measurement due to chromatography effect of macromolecules. In the Fig. 10, the signals of *m/z* 47, 63, and 64 can be assigned to OP<sup>+</sup>, O<sub>2</sub>P<sup>+</sup> and HO<sub>2</sub>P<sup>+</sup> produced from degradation of DOPO-POSS in EP-3. These data were supported by the TGA-FTIR analysis.

Associating with the pyrolysis products that have been discussed, the oversimplified fragments of EP-3 are shown in the Scheme 3. It can be found that the degradation of EP-3 can be divided into two steps. At the beginning, the degradation is mainly attributed to the alkyl chain and polyol in the crosslink network. With raising temperature, some aromatic molecules and phosphorous-containing groups in the EP-3 are decomposed.

### 3.5. FTIR analysis of pyrolysis residues of EP-3

FTIR spectra of EP-3 and its solid products of thermal decomposition collected in thermogravimetry at 25%, 50%, and 75% weight-loss are shown in Fig. 11. It can be seen that peaks at 3200–3600, 3055, 2868–2962, 1602, 1504, 1455, 1226, 1025, 1178, and 825 cm<sup>-1</sup> are the characteristic absorption of EP networks [1,6]. The origins of absorption in EP networks are outlined in Fig. 12. Moreover, the P–O–phenyl stretching vibration at 909 cm<sup>-1</sup> and the C–H deformation vibration of phenyl rings of DOPO groups at 755 cm<sup>-1</sup> from DOPO-POSS are identified [31,32].

After 25% weight-loss of EP-3, there is a decrease in the intensity of the –OH and –NH related bonds (3200–3600 cm<sup>-1</sup>) and alkyl ether bonds (1103 cm<sup>-1</sup>), indicating preferential decomposition of the 2-hydroxytrimethylene and its fragments along with the bisphenol A unit. Simultaneously, the aliphatic components absorption at 1293 cm<sup>-1</sup> decreases obviously.



**Scheme 3.** Oversimplified fragments of EP-3.



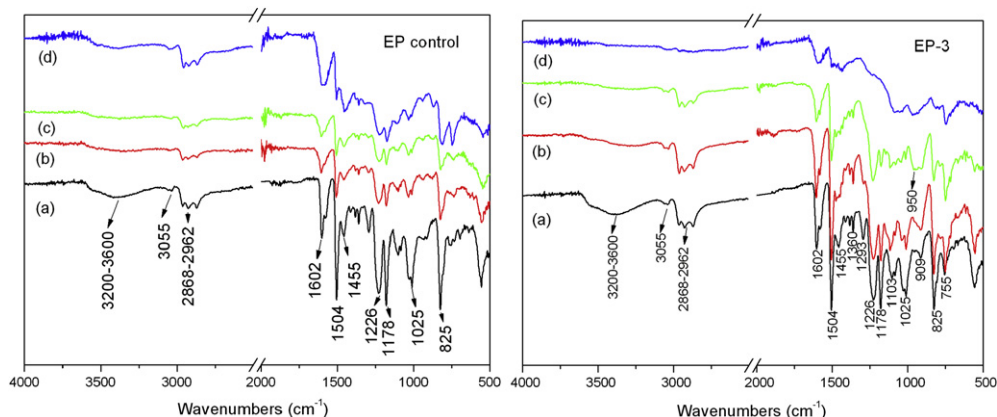


Fig. 11. FTIR spectra of the condensed phase of EP control and EP-3: initial (a), 25% weight-loss (b), 50% weight-loss (c), 75% weight-loss (d).

After 50% weight-loss of EP-3, significant modifications in the epoxy networks are observed. There is a decrease in the intensity of the absorption of aliphatic components (2962–2868, 1386, 1360, and 1178  $\text{cm}^{-1}$ ) and alkyl–aryl ether bonds (1260 and 1025  $\text{cm}^{-1}$ ). It indicates the decomposition of the isopropyl group and alkyl–aryl ether in the bisphenol A unit. Moreover, a new absorption at 950  $\text{cm}^{-1}$  is observed after 50% weight-loss of EP-3. This new absorption could be assigned to Si–O–phenyl and P–O–phenyl stretching vibration, which has been reported in previous papers [34,35].

After 75% weight-loss of EP-3, dramatic changes are noticed in all the spectral regions. The absorption of aliphatic components disappears totally. The aromatic ring C=C stretching vibration at 1504  $\text{cm}^{-1}$  disappears and that at 1590 and 1434  $\text{cm}^{-1}$  becomes broader, indicating the formation of polyaromatic carbons. Moreover, the broad absorption at 1080  $\text{cm}^{-1}$  indicates the formation of  $\text{SiO}_2$ . The Si–O–phenyl and P–O–phenyl stretching vibrations around 950  $\text{cm}^{-1}$  become broader and stronger, indicating the reactions between DOPO-POSS and epoxy resin under pyrolysis. These reactions are trusted that it would enhance the formation of char, which have superior thermal stability.

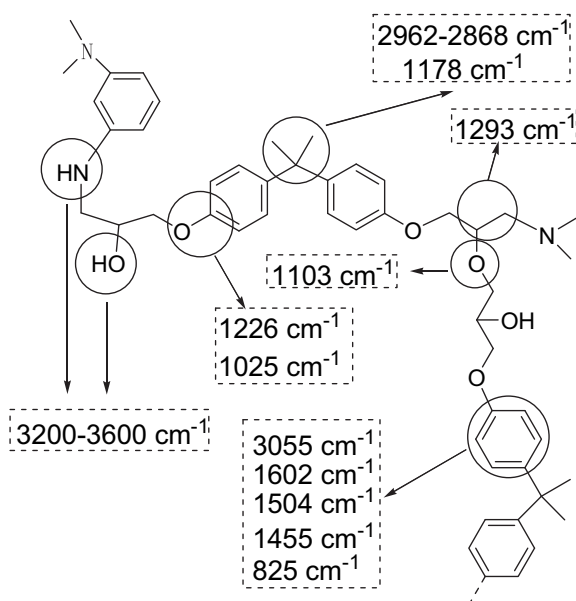


Fig. 12. The origin of main absorbance bands observed in the FTIR spectra.

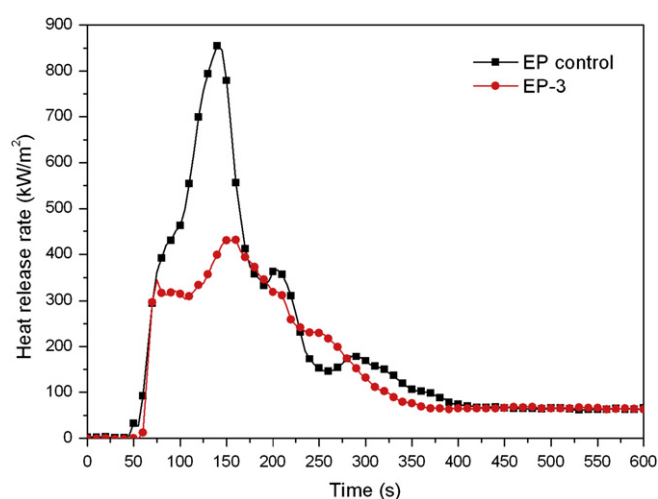


Fig. 13. Heat release rate (HRR) of the EP control and EP-3.

### 3.6. Fire behaviours of EP composites

To evaluate the fire performance of DOPO-POSS/EP composites, cone calorimeter test was carried out. The cone calorimeter enables quantitative analysis of the flammability of materials through providing parameters such as heat release rate (HRR), peak of heat release rate (PHRR), time to ignition (TTI), and total heat released (THR). Experimental results obtained by cone calorimeter for EP control and EP-3 are summarized in Table 5 and Fig. 13.

As shown in Fig. 13, the fire behaviour is clearly modified by the presence of the DOPO-POSS. A significant decrease (almost 50%) is observed in the peak of heat release rate which is a major parameter in controlling flame propagation of fire [36]. Moreover, two small peaks of heat release rate during the combustion processes of EP control are observed at about 210 s and 300 s, respectively. It indicates that the char of EP control could be destroyed during the combustion process. However, the HRR curve of EP-3 is smooth and

Table 5  
Cone calorimeter data for the EP control and EP-3.

Composites	EP control	EP-3
TTI (s)	45	57
PHRR ( $\text{kW/m}^2$ )	855	431
THR ( $\text{MJ/m}^2$ )	118	91

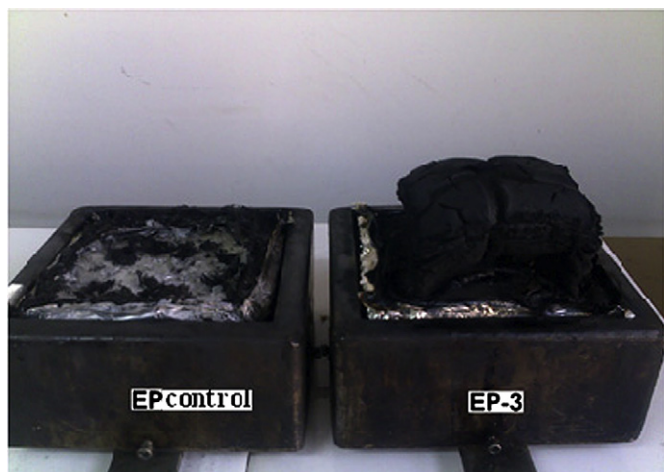


Fig. 14. Photographs of chars from EP control and EP-3 after cone calorimeter tests.

decreases gradually. It shows that DOPO-POSS is helpful to the formation of a char layer which is more firm and has higher thermo-stability. In Table 5, the TTI of EP-3 is also slightly increased and the THR of EP-3 reduced markedly with DOPO-POSS load.

After the cone calorimeter test, some interesting information is found by the visual observation of the end of test residues (Fig. 14). There is no obvious char of EP control could be observed, whereas, a char layer of EP-3 which is intumescent and firm is created during the combustion. Remarkable reduction of HRR values observed for

EP-3 is likely to be due to the presence of this char layer which has higher thermo-stability. The char layer generated is thought to act as a barrier for both heat flow and mass transport [37].

### 3.7. Morphological analysis of the char

Fig. 15 shows the SEM photographs obtained for exterior and interior char residues of the EP control and EP-3 samples. It is not difficult to discern the differences of the chars between the exterior and interior of the EP control. The char of EP control presents a continual char layer which has many micro-sized cracks and pits on it. As shown in the fire behaviours section, little char remain was observed after cone calorimeter test, which indicates the weakly thermo-stability of the char of EP control.

The exterior char of EP-3 sample presents a continual and rugged char layer. The interior char of EP-3 present micro-structures of thin char layers and small pores. This phenomenon could attribute to increase of the viscosity of thermal degradation products which could swell during the gas release. The intumescent and firm char of EP-3 indicates that the incorporation of DOPO-POSS could enhance the thermo-stability of the char efficiently.

### 3.8. XPS analysis of the char

The exterior and interior char of the EP control and EP-3 were investigated by XPS analysis. The  $C_{1s}$ ,  $O_{1s}$ ,  $Si_{2p}$ , and  $P_{2p}$  spectra of exterior char of the EP-3 are shown in Fig. 16. As shown in Fig. 16, four bands are observed from  $C_{1s}$  spectra: the peak at around 284.6 eV is attributed to C–H and C–C in aliphatic and aromatic

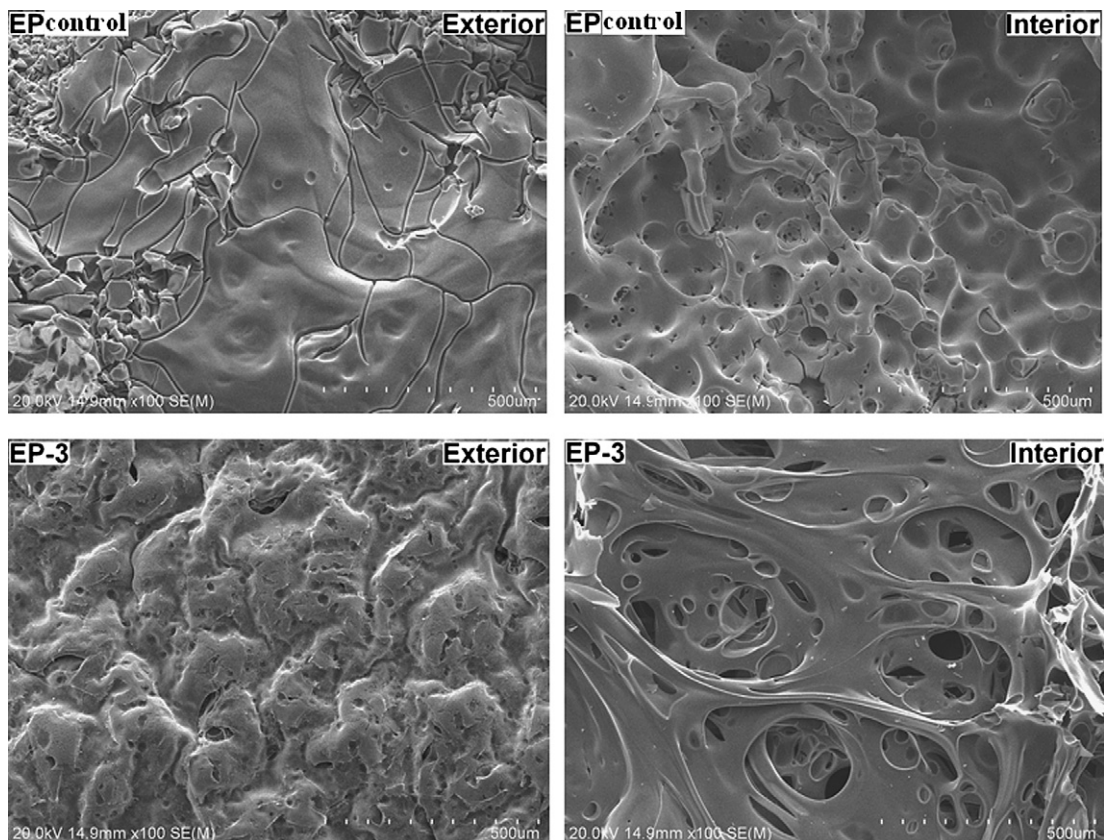


Fig. 15. Residue morphologies of EP control and EP-3.

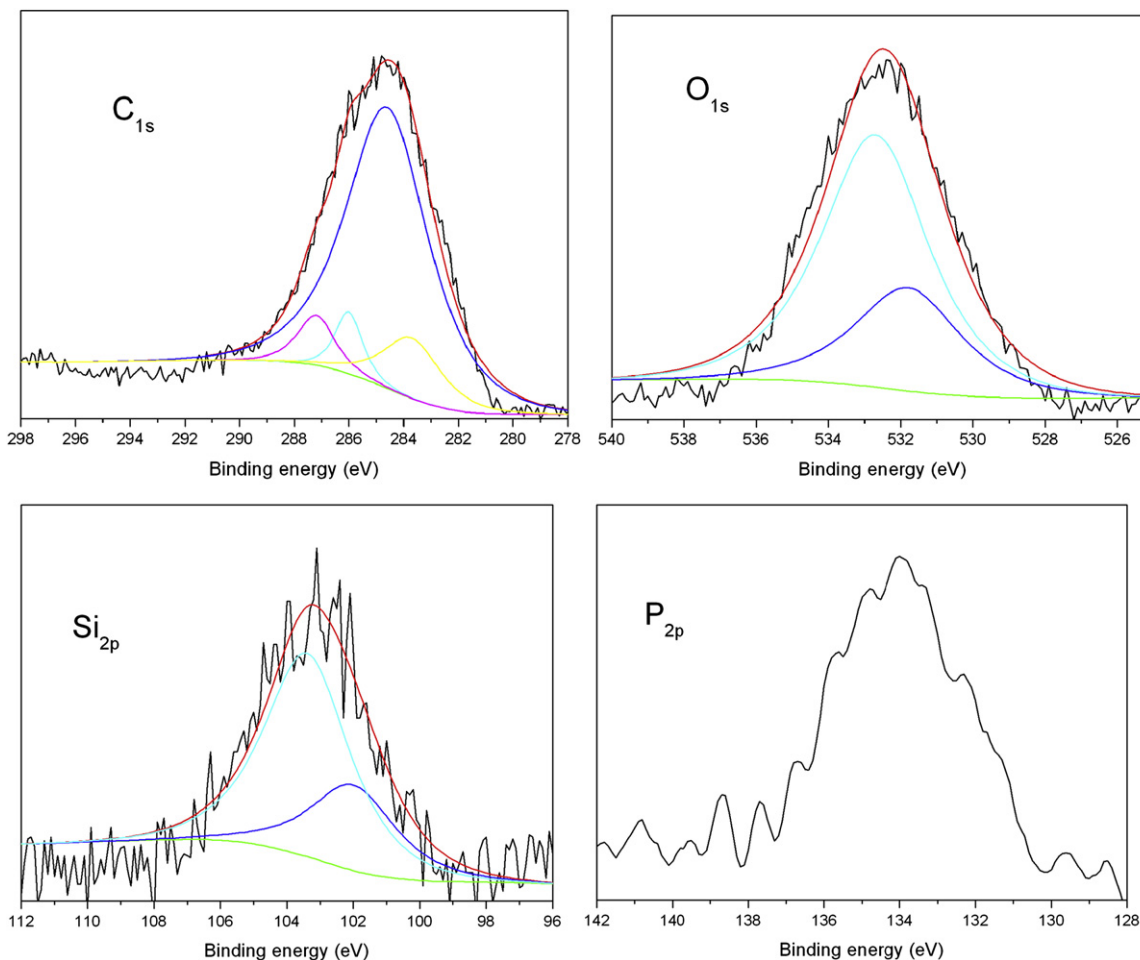


Fig. 16.  $C_{1s}$ ,  $O_{1s}$ ,  $Si_{2p}$ , and  $P_{2p}$  XPS spectra of the char of EP-3.

species, the peak at around 286.0 eV is assigned to C–O in ether and/or hydroxyl groups, the peak at around 287.2 eV corresponds to carbonyl groups, another peak at around 283.7 eV is assigned to C–Si band [10,35]. The  $O_{1s}$  spectra have two peaks at around 531.5 and 532.8 eV. It is reported that the peak at 531.5 eV can be attributed to the =O in phosphate or carbonyl groups and the peak at 532.8 eV is assigned to –O– in C–O–C, Si–O–C, and P–O–C groups [35]. The  $Si_{2p}$  spectra have two peaks at around 102.0 and 103.4 eV. It is reported that the peak at 102.0 eV can be assigned to  $RSiO_{1.5}$  or Si–C in the char and the peak at 103.4 eV is attribute to Si– $O_2$  and Si–O in the char [10,35]. The weak peak at around 134.0 eV in  $P_{2p}$  spectra can be assigned to the pyrophosphate and polyphosphate [1]. These results mean that lots of  $SiO_2$ , Si–O–phenyl, pyrophosphate, and polyphosphate structures are created in the char of EP-3 after the cone calorimeter test. It indicates that DOPO-POSS have an obvious action in the condensed phase.

**Table 6**  
XPS results of the chars of EP control and EP-3.

Elements	Element concentration (%)			
	EP control (exterior)	EP control (interior)	EP-3 (exterior)	EP-3 (interior)
C	79	81	59	60
O	19	18	33	31
N	2	2	2	3
Si	0	0	5	5
P	0	0	1	1

The concentrations of C, O, N, Si, and P in exterior and interior char of the EP control and EP-3 are listed in Table 6. The atom percent of C element in the char of EP-3 is lower than that in the EP control and the atom percent of O element in the char of EP-3 is higher than that in the EP control. The reason is that the exterior char is highly oxidized under the rich oxygen condition. Moreover, a number of Si– $O_2$  and P–O structures are kept in the char, which is another reason to lead higher O element in the char of EP-3. A number of Si and P element are observed in the char of EP-3, which is helpful to the enhancement of the thermo-stability of the char [8]. The presence of Si and P element in char of the EP control probably is derived from the cone calorimeter test.

#### 4. Conclusions

Flame-retarded epoxy resin (EP) composites have been obtained by incorporation of a novel polyhedral oligomeric silsesquioxane containing 9,10-dihydro-9-oxa-10-phosphaphenanthrene-10-oxide (DOPO-POSS) into EP. The hydroxyl group of DOPO-POSS and the epoxy group of DGEBA could pre-react, according to FTIR analysis, which is helpful to improve the compatibility of the DOPO-POSS with EP. The nano-scale dispersion of DOPO-POSS in the composites was observed by SEM. An increase of  $T_g$  of the EP composites with DOPO-POSS loading was confirmed by DSC; this improvement may be attributed to the pre-reaction. The decomposition temperatures and the evolved gaseous products were investigated in detail by TGA, TGA-FTIR, and TGA-MS. Increases of



thermal stability and char yield were observed by TGA analysis. Phosphorous volatiles were discovered using TGA-FTIR and TGA-MS. Associating with the pyrolysis products observed, the decomposition reaction pathways of EP composites were suggested. The characteristic absorbances of SiO<sub>2</sub>, Si–O, and P–O structures were observed in the char of EP-3 by FTIR. These results indicate that DOPO-POSS have significant interaction with EP networks in the condensed phase. The increased char yield and the release of compounds containing phosphorus crucially improve the flame retardancy of the EP composites. The fire behaviour of EP composites evaluated by cone calorimetry indicate that DOPO-POSS can reduce the HRR of EP composite significantly and accelerate the formation of char layer. The chars of EP composites after cone calorimeter test were investigated by SEM and XPS. These results explain the flame retardancy mechanisms of DOPO-POSS in condensed phase.

### Acknowledgements

This work was funded by National High Technology Research and Development Program 863 (No. 2007AA03Z538), which is highly appreciated.

### References

- Wang X, Hu Y, Song L, Xing WY, Lu HD, Lv P, et al. Flame retardancy and thermal degradation mechanism of epoxy resin composites based on a DOPO substituted organophosphorus oligomer. *Polymer* 2010;51:2435–45.
- Liu HZ, Zheng SX, Nie KM. Morphology and thermomechanical properties of organic–inorganic hybrid composites involving epoxy resin and an incompletely condensed polyhedral oligomeric silsesquioxane. *Macromolecules* 2005;38:5088–97.
- Brus J, Urbanová M, Strachota A. Epoxy networks reinforced with polyhedral oligomeric silsesquioxane: structure and segmental dynamics as studied by solid-state NMR. *Macromolecules* 2008;41:372–86.
- Liu R, Wang XD. Synthesis, characterization, thermal properties and flame retardancy of a novel nonflammable phosphazene-based epoxy resin. *Polym Degrad Stab* 2009;94:617–24.
- Wu K, Song L, Hu Y, Lu HD, Kandola BK, Kandare E. Synthesis and characterization of a functional polyhedral oligomeric silsesquioxane and its flame retardancy in epoxy resin. *Prog Org Coat* 2009;65:490–7.
- Schartel B, Balabanovich AI, Braun U, Knoll U, Artner J, Ciesielski M, et al. Pyrolysis of epoxy resins and fire behavior of epoxy resin composites flame-retarded with 9,10-dihydro-9-oxa-10-phosphaphenanthrene-10-oxide additives. *J Appl Polym Sci* 2007;104:2260–9.
- Nagendiran S, Alagar M, Hamerton I. Octasilsesquioxane-reinforced DGEBA and TGDDM epoxy nanocomposites: characterization of thermal, dielectric and morphological properties. *Acta Mater* 2010;58:3345–56.
- Chow WS, Neoh SS. Dynamic mechanical, thermal, and morphological properties of silane-treated montmorillonite reinforced polycarbonate nanocomposites. *J Appl Polym Sci* 2009;114:3967–75.
- Becker L, Lenoir D, Matuschek G, Ketrup A. Thermal degradation of halogen-free flame retardant epoxides and polycarbonate in air. *J Anal Appl Pyrolysis* 2001;60:55–67.
- Su C-H, Chiu Y-P, Teng C-C, Chiang C-L. Preparation, characterization and thermal properties of organic–inorganic composites involving epoxy and polyhedral oligomeric silsesquioxane (POSS). *J Polym Res* 2010;17:673–81.
- Laine RM. Nanobuilding blocks based on the [OSiO<sub>1.5</sub>]<sub>k</sub> (x = 6, 8, 10) octasilsesquioxanes. *J Mater Chem* 2005;15:3725–44.
- Li GZ, Wang LC, Ni HL, Pittman CU. Polyhedral oligomeric silsesquioxane (POSS) polymers and copolymers: a review. *J Inorg Organomet Polym* 2001;11:123–54.
- Liu L, Hu Y, Song L, Nazare S, He SQ, Hull R. Combustion and thermal properties of octaTMA-POSS/PS composites. *J Mater Sci* 2007;42:4325–33.
- Vannier A, Duquesne S, Bourbigot S, Castrovinci A, Camino G, Delobel R. The use of POSS as synergist in intumescent recycle poly(ethylene terephthalate). *Polym Degrad Stab* 2008;93:818–26.
- Baney RH, Itoh M, Sakakibara A, Suzuki T. Silsesquioxanes. *Chem Rev* 1995;95:1409–30.
- Zhang WA, Fang B, Walther A, Müller AHE. Synthesis via RAFT polymerization of tadpole-shaped organic/inorganic hybrid Poly(acrylic acid) containing polyhedral oligomeric silsesquioxane (POSS) and their self-assembly in water. *Macromolecules* 2009;42:2563–9.
- Zhang ZP, Liang GZ, Lu TL. Synthesis and characterization of cage octa(aminopropyl)silsesquioxane. *J Appl Polym Sci* 2007;103:2608–14.
- Pellice SA, Fasce DP, Williams RJ. Properties of epoxy networks derived from the reaction of diglycidyl ether of bisphenol A with polyhedral oligomeric silsesquioxanes bearing OH-functionalized organic substituents. *J Polym Sci Pol Phys* 2003;41:1451–61.
- Liu HZ, Zhang WA, Zheng SX. Montmorillonite intercalated by ammonium of octaaminopropyl polyhedral oligomeric silsesquioxane and its nanocomposites with epoxy resin. *Polymer* 2005;46:157–65.
- Lejeune N, Dez I, Jaffres PA, Lohier JF, Madec PJ, Sopkova-de Oliveira Santos J. Synthesis, crystal structure and thermal properties of phosphorylated cyclo-triphosphazenes. *Eur J Inorg Chem* 2008;1:138–43.
- Orme CJ, Klaehn JR, Harrup MK, Lash RP, Stewart FF. Characterization of 2-(2-methoxyethoxy)ethanol-substituted phosphazene polymers using pervaporation, solubility parameters, and sorption studies. *J Appl Polym Sci* 2005;97:939–45.
- Zhu L, Zhu Y, Pan Y, Huang YW, Huang XB, Tang XZ. Fully crosslinked poly [cyclo-triphosphazene-co-(4,4'-sulfonyldiphenol)] microspheres via precipitation polymerization and their superior thermal properties. *Macromol React Eng* 2007;1:45–52.
- Wang X, Hu Y, Song L, Xing WY, Lu HD. Thermal degradation behaviors of epoxy resin/POSS hybrids and phosphorus–silicon synergism of flame retardancy. *J Polym Sci Pol Phys* 2010;48:693–705.
- Lin HT, Lin CH, Hu YM, Su WC. An approach to develop high-Tg epoxy resins for halogen-free copper clad laminates. *Polymer* 2009;50:5685–92.
- Liu WS, Wang ZG, Xiong L, Zhao LN. Phosphorus-containing liquid cycloaliphatic epoxy resins for reworkable environment-friendly electronic packaging materials. *Polymer* 2010;51:4776–83.
- Lin CH, Feng CC, Hwang TY. Preparation, thermal properties, morphology, and microstructure of phosphorus-containing epoxy/SiO<sub>2</sub> and polyimide/SiO<sub>2</sub> nanocomposites. *Eur Polym J* 2007;43:725–42.
- Zhong HF, Wei P, Jiang PK, Wang GL. Thermal degradation behaviours and flame retardancy of PC/ABS with novel silicon-containing flame retardant. *Fire Mater* 2007;31:411–23.
- Lu SY, Hamerton I. Recent developments in the chemistry of halogen-free flame retardant polymers. *Prog Polym Sci* 2002;27:1661–712.
- Schartel B, Braun U, Balabanovich AI, Artner J, Ciesielski M, Döring M, et al. Pyrolysis and fire behaviour of epoxy systems containing a novel 9,10-dihydro-9-oxa-10-phosphaphenanthrene-10-oxide (DOPO)-based diamino hardener. *Eur Polym J* 2008;44:704–15.
- Artner J, Ciesielski M, Walter O, Döring M, Perez RM, Sandler JKW, et al. A novel DOPO-Based Diamine as hardener and flame retardant for epoxy resin systems. *Macromol Mater Eng* 2008;293:503–14.
- Zhang WC, Li XM, Guo XY, Yang RJ. Mechanical and thermal properties and flame retardancy of phosphorus-containing polyhedral oligomeric silsesquioxane (DOPO-POSS)/polycarbonate composites. *Polym Degrad Stab* 2010;95:2541–6.
- Zhang WC, Yang RJ. Synthesis of phosphorus-containing polyhedral oligomeric silsesquioxanes via hydrolytic condensation of a modified silane. *J Appl Polym Sci*. doi:10.1002/app.34471.
- Pawlowski KH, Schartel B. Flame retardancy mechanisms of triphenyl phosphate, resorcinol bis(diphenyl phosphate) and bisphenol A bis(diphenyl phosphate) in polycarbonate/acrylonitrile-butadiene-styrene blends. *Polym Int* 2007;56:1404–14.
- Perret B, Schartel B. The effect of different impact modifiers in halogen-free flame retarded polycarbonate blends – I. Pyrolysis. *Polym Degrad Stab* 2009;94:2194–203.
- Song L, He QL, Hu Y, Chen H, Liu L. Study on thermal degradation and combustion behaviours of PC/POSS hybrids. *Polym Degrad Stab* 2008;93:627–39.
- Franchini E, Galy J, Gérard J-F, Tabuani D, Medici A. Influence of POSS structure on the fire retardant properties of epoxy hybrid networks. *Polym Degrad Stab* 2009;94:1728–36.
- Feng J, Hao JW, Du JX, Yang RJ. Flame retardancy and thermal properties of solid bisphenol A bis(diphenyl phosphate) combined with montmorillonite in polycarbonate. *Polym Degrad Stab* 2010;95:2041–8.